Electronic Supplementary Material (ESI) for Materials Advances.

Supporting information

A non-covalent supramolecular dual-network polyelectrolyte evaporator based on direct-ink-writing for stable solar thermal evaporation

Sihan Tang,[a] Xinyue Lu,[a] Peng Geng,[a] Daobing Chen,[a] Yunsong Shi,[c] Jin Su,[a] Yan Zhou,*[b] Bin Su,*[a] Shifeng Wen.*[a]

a State Key Laboratory of Materials Processing and Die & Mold Technology, School of Materials Science and Engineering, Huazhong University of Science and Technology, Wuhan 430074, China

b Department of Construction Management, School of Civil & Hydraulic Engineering, Huazhong University of Science and Technology, Wuhan 430074, China

c Department of Orthopaedics, Union Hospital, Tongji Medical College, Huazhong University of Science and Technology, Wuhan 430022, China

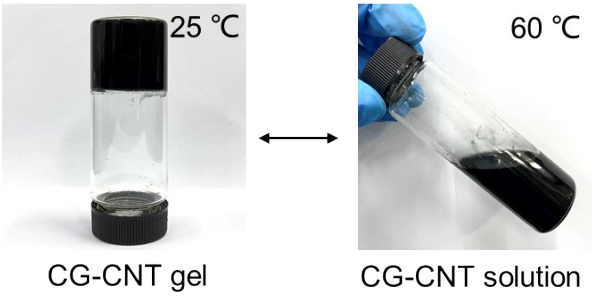

Fig. S1. CG-CNT ink has a typical thermo sensitive property which is soluble at 60°C while turning to gel at room temperature (25°C).

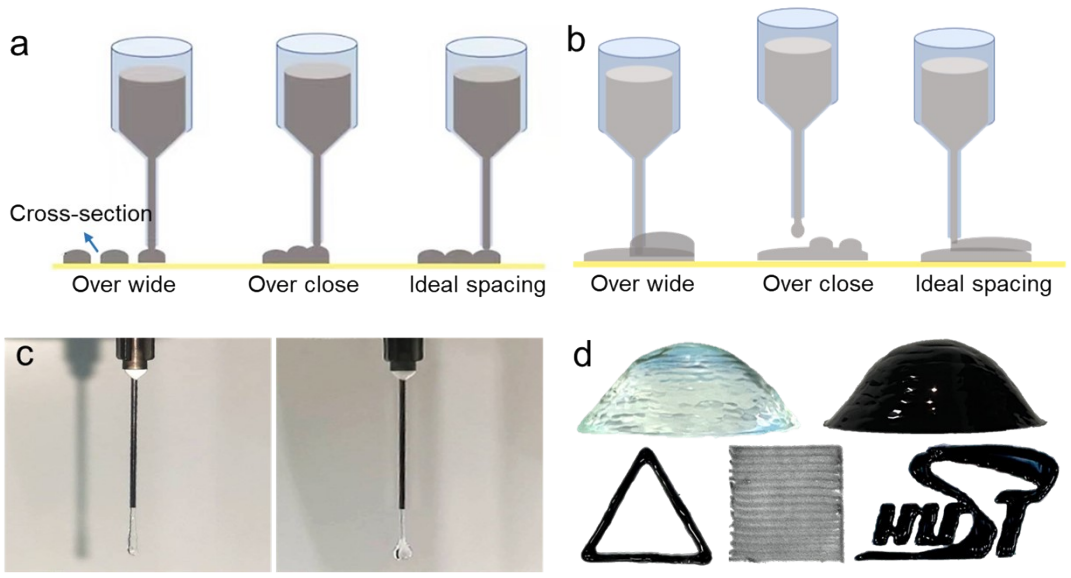

Fig. S2. Different extrusion states of DIW ink: Effect of line distance (a) and layer distance (b) on printing. (c) Effect of gelation rate on ink extrusion, the ideal state should be continuous and uniform filament (left). (d) Optical pictures of printed CG and CG-CNT.

Table S1 Summary of the different printing parameters.

Concentration of ink (wt%)	Nozzle size (mm)	Printing speed (mm/s)	Extrusion speed (mm/s)	Line distance (mm)	Layer distance (mm)
1.5	0.40	10.00	2.60	0.50	0.50
2.0	0.60	10.00	4.70	0.70	1.00
2.5	0.60	10.00	9.15	1.00	1.00
3.0	0.84	10.00	6.67	1.00	1.00

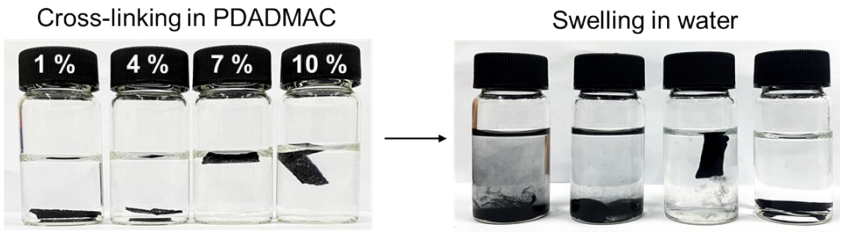

Fig. S3. Swelling test of CG-CNT (freeze-dried) with different concentrations of PDADMAC, respectively.

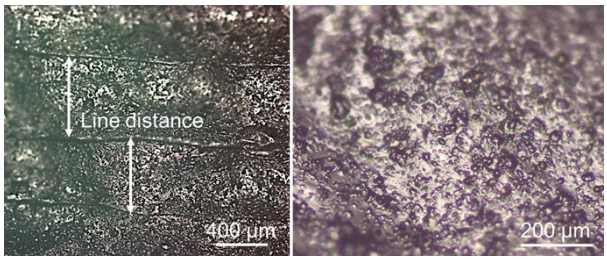

Fig. S4. Optical microscope images of freeze-dried CGP-CNT.

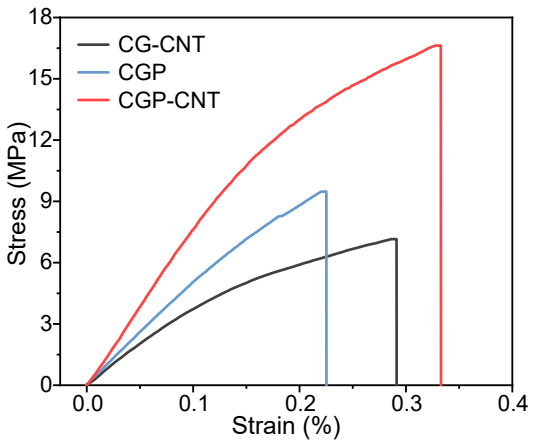

Fig. S5. Tensile stress-strain curves of CG-CNT, CGP and CGP-CNT aerogels.

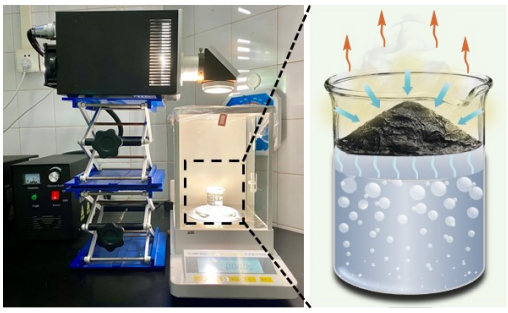

Fig. S6. Digital images and of solar thermal evaporation instrument.

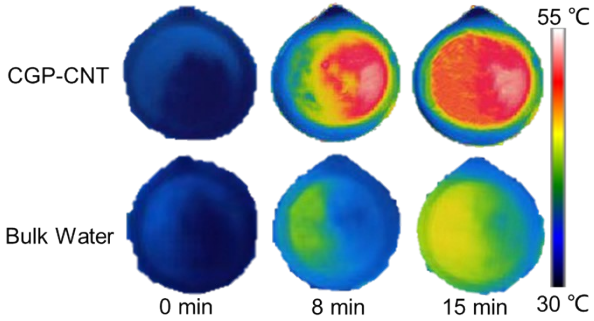

Fig. S7. Infrared images of CGP-CNT and bulk water under 1 sun irradiation.

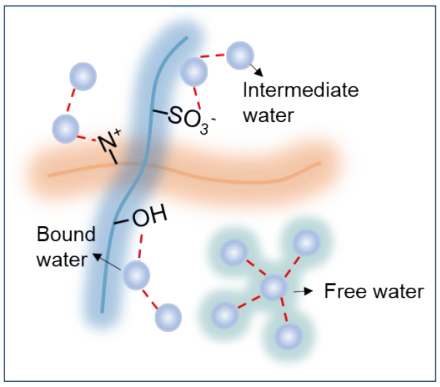

Fig. S8. States of water and hydrogen bonds around polymer chains.

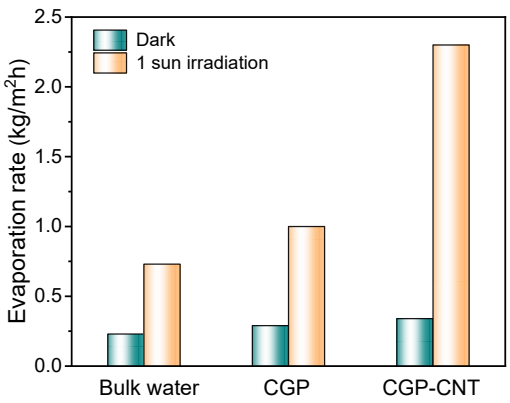

Fig. S9. Evaporation rate of bulk water, CGP and CGP-CNT in dark and 1 sun irradiation, respectively.

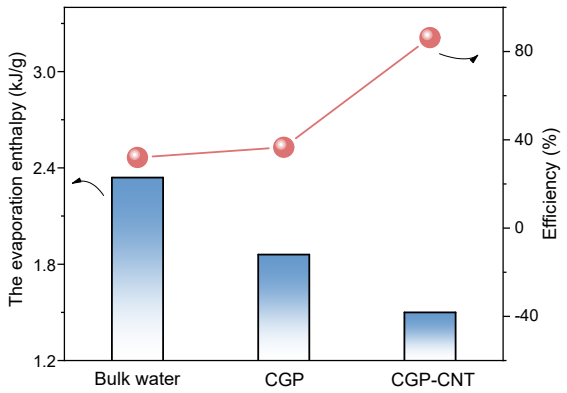

Fig. S10. The evaporation enthalpy and efficiency of bulk water, CGP and CGP-CNT under 1 sun irradiation.

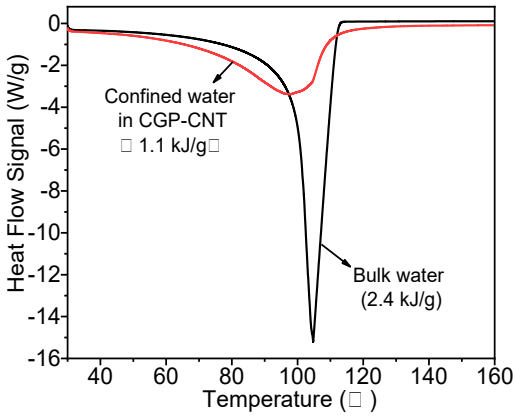

Fig. S11. DSC curves of confined water in CGP-CNT compared to bulk water.

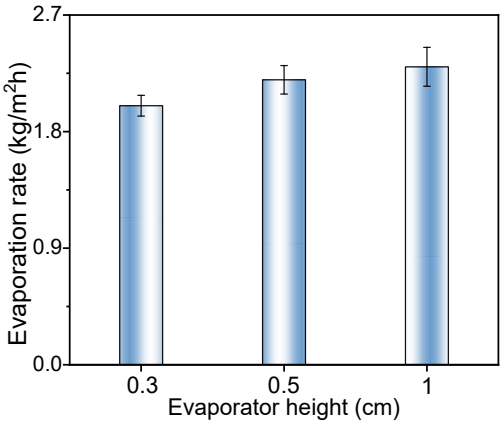

Fig. S12. Effect of evaporator height on evaporation rate (D=3 cm).

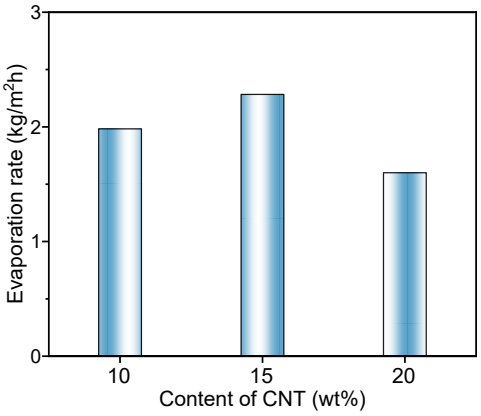

Fig. S13. The effect of different CNT contents on the solar thermal evaporation performance under one sun irradiation. (Note: The content of CNT was relative to the mass of CG.)

Table S2 Comparation of the evaporation rate of CGP-CNT with some recent reports.

Entry	Evaporation rate ($kg \cdot m^{-2} \cdot h^{-1}$)	Efficiency (%)	Reference in supporting information
1	**2.3**	**87**	**This work**
2	2.1	95	[1]
3	1.45	94.5	[2]
4	1.27	87.5	[3]
5	1.25	85.6	[4]
6	1.723	107.8	[5]
7	2.4	98	[6]
8	2.17	99.7	[7]
9	1.57	88.38	[8]
10	1.33	90.6	[9]

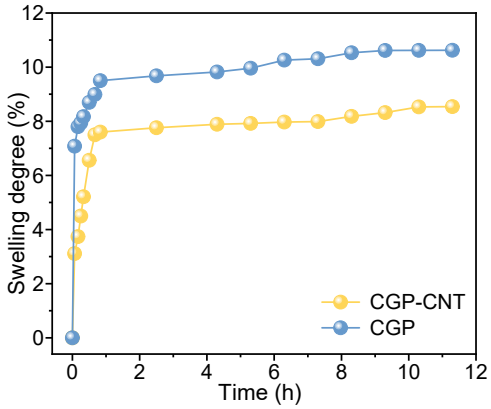

Fig. S14. Curves of CGP-CNT and CGP swelling degree with time in water.

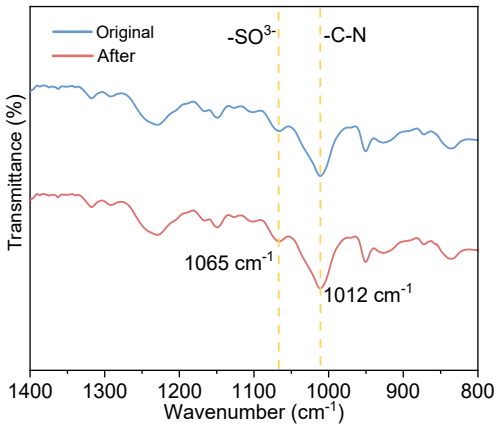

Fig. S15. FTIR curves of CGP-CNT after evaporation compared to original.

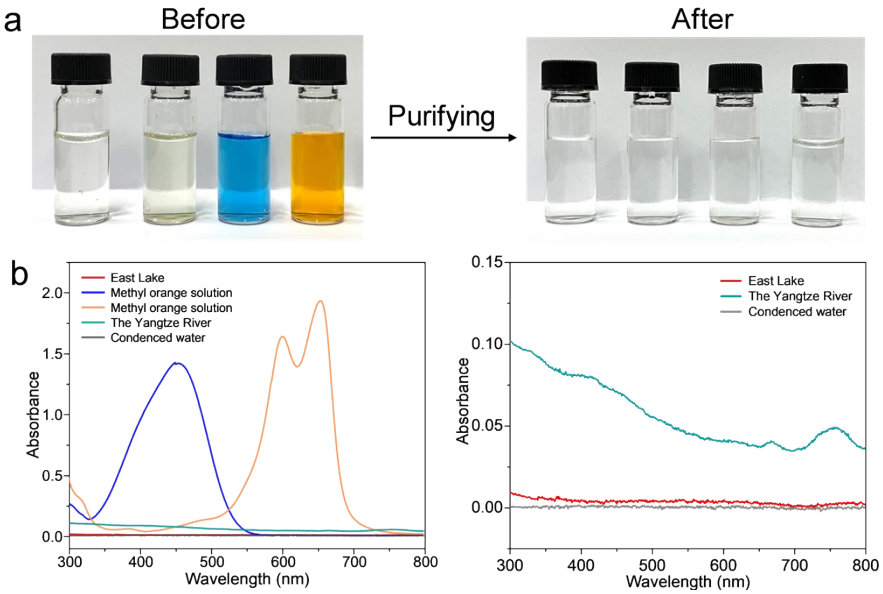

Fig. S16. Optical pictures (a) and UV-vis-NIR absorption spectra (b) of different water samples after evaporation, respectively.

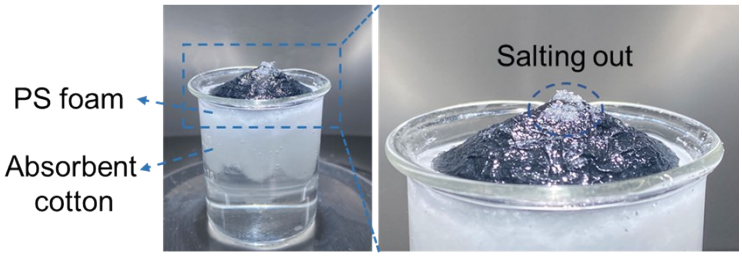

Fig. S17. Optical pictures of CGP-CNT evaporation.

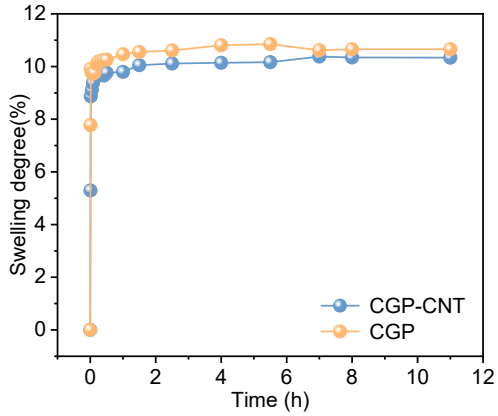

Fig. S18. Curves of CGP-CNT and CGP swelling degree with time in seawater.

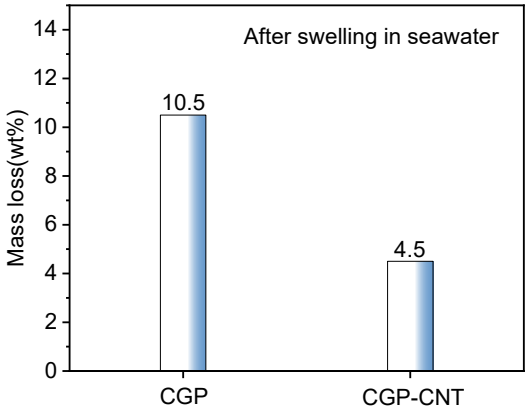

Fig. S19. Mass loss of CGP-CNT and CGP in seawater.

Table S3 Composition of CGP-CNT after swelling in water and seawater, respectively.

Conditions		N:S (mol)
After swelling in water	interior	0.772
	exterior	0.787
After swelling in seawater	interior	0.755
	exterior	0.765

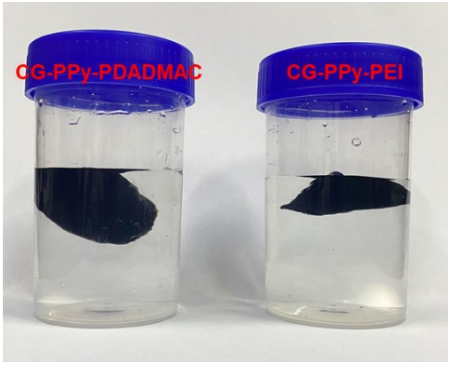

Fig. S20. Optical pictures of CG-PPy-PDADMAC and CG-PPy-PEI in water, respectively.

Preparation: 2.04 g of CG and 0.306 g PPy (Polypyrrole) were dissolved in 100 mL H_2O, then stirred in a 60°C water bath (600 rpm) and sonicated for 1 h to form a homogeneous, black CG-PPy ink. CG-PPy-PEI and CG-PPy-PDADMAC were prepared using the same experiments procedure in the main text.

References

1 P. Zhang, Q. Liao, H. Yao, H. Cheng, Y. Huang, C. Yang, L. Jiang and L. Qu, *J. Mater. Chem. A*, 2018, **6**, 15303-15309.
2 Z. Wang, H. Liu, F. Chen and Q. Zhang, *J. Mater. Chem. A*, 2020, **8**, 19387-19395.
3 Y. Li, T. Gao, Z. Yang, C. Chen, Y. Kuang, J. Song, C. Jia, E. M. Hitz, B. Yang and L. Hu, *Nano Energy*, 2017, **41**, 201-209.
4 Y. Li, T. Gao, Z. Yang, C. Chen, W. Luo, J. Song, E. Hitz, C. Jia, Y. Zhou, B. Liu, B. Yang and L. Hu, *Adv. Mater.*, 2017, **29**, 1700981.
5 N. Cao, S. Lu, R. Yao, C. Liu, Q. Xiong, W. Qin and X. Wu, *Chem. Eng. J.*, 2020, **397**, 125522.
6 W. Jonhson, X. Xu, D. Zhang, W. T. Chua, Y. H. Tan, X. Liu, C. Guan, X. H. Tan, Y. Li, T. S. Herng, J. C. Goh, J. Wang, H. He and J. Ding, *ACS Appl. Mater. Inter.*, 2021, **13**, 23220-23229.
7 Y. Yang, W. Fan, S. Yuan, J. Tian, G. Chao and T. Liu, *J. Mater. Chem. A*, 2021, **9**, 23968-23976.
8 J. Yang, H. Wang, B. Zhou, J. Shen, Z. Zhang and A. Du, *Langmuir*, 2021, **37**, 2129-2139.
9 J. Yuan, X. Lei, C. Yi, H. Jiang, F. Liu and G. J. Cheng, *Chem. Eng. J.*, 2022, **430**, 132765.